Int. J. Heat Mass Transfer. Vol. 16, pp. 1385–1396. Pergamon Press 1973. Printed in Great Britain

TURBULENT HEAT TRANSFER AND THE PERIODIC VISCOUS SUBLAYER

RONALD L. MEEK* and ALVA D. BAER
Department of Chemical Engineering, University of Utah, Salt Lake City, Utah, U.S.A.

(*Received* 13 *August* 1971 *and in revised form* 30 *October* 1972)

Abstract—Heat transfer calculations based on the fluctuating viscous sublayer model of turbulent flow are presented which incorporate two essential but heretofore neglected features of the real flow situation; namely, that the sublayer fluctuations impose wall temperature fluctuations and that on average the sublayer does not decay completely to the wall but rather there exists a maximum turbulence penetration thickness. The resulting temperature distributions and heat transfer coefficients are in agreement with empirical correlations of the experimental data for Prandtl numbers greater than one. Heat transfer to liquid metals is also considered (Prandtl number much less than one) and computed heat transfer coefficients are 25–50 per cent higher than published correlations of empirical data. The computations indicate that for liquid metals the Nusselt number is not a single valued function of the Péclét number.

NOMENCLATURE

c, heat capacity of fluid;
D, tube diameter;
g, arbitrary function;
h, local heat transfer coefficient based on bulk fluid temperature;
k, thermal conductivity of fluid; k_t, thermal conductivity by a turbulent mechanism;
n, an integer;
N_{Nu}, local Nusselt number, hD/k;
N_{Pe}, Péclét number, $N_{Re}N_{Pr}$;
N_{Pr}, Prandtl number, $c\mu/k$;
N_{Re}, Reynolds number, $D\langle u_z\rangle/\nu$;
N_{St}, Stanton number, $N_{Nu}/N_{Re}N_{Pr}$;
q, heat flux; $\bar{q}_w$, time averaged heat flux at the wall;
R, tube radius, $R^+ = Ru_*/\nu$;
t, time, $t^+ = u_*(t/\nu)^{1/2}$;
T, sublayer growth period; $T^+ = u_*(T/\nu)^{\frac{1}{2}}$;
u, velocity $\langle u_z\rangle$, bulk velocity in axial direction; u_B, velocity at outer edge of growing sublayer; $\bar{u}$, time average velocity; u_*, friction velocity, $(\bar{\tau}_w/\rho)^{\frac{1}{2}}$; $u^+ = u/u_*$;
x,y,z, rectangular cartesian coordinates relative to a point on the wall in the transverse, normal, and axial direction of a tube respectively; $y^+ = yu_*/\nu$;
α, thermal diffusivity of fluid, $k/\rho c$; α_s, thermal diffusivity of wall material; αt, eddy diffusivity for energy transport;
Γ, thermal responsivity of fluid, $(k\rho c)^{\frac{1}{2}}$; Γ_s, thermal responsivity of wall material;
δ, sublayer thickness; $\delta^+ = \delta u_*/\nu$; δ_M, maximum thickness of sublayer growth; δ_1, minimum sublayer decay thickness; δ_T, thermal boundary layer thickness;
ε, an infinitesimal;
θ, temperature; θ_i, constant temperature at outer edge of thermal sublayer; $\langle\theta\rangle$, bulk fluid temperature; $\bar{\theta}_w$, time averaged wall temperature; θ^+, dimensionless temperature, $(\theta - \bar{\theta}_w)\rho c u_*/\bar{q}_w$; θ'_w, wall temperature fluctuation;
κ, first constant from mixing length theory $\equiv 0{\cdot}4$;
μ, viscosity;
ν, kinematic viscosity; ν_t, eddy diffusivity for momentum transport;
ρ, density;

* Bell Telephone Laboratories, Murray Hill, N.J., U.S.A.

τ, momentum flux (or shear stress); $\bar{\tau}_w$, time averaged momentum flux at the wall.

INTRODUCTION

SOLUTION of turbulent transport problems is frustrated by our inability to adequately describe the turbulent flow itself. Thus, while there are many semi-theoretical and empirical correlations of the experimental data for a number of common situations, prediction of coefficients in new situations or for combined transport is often hazardous. Some years ago, Einstein and Li [1] proposed a periodic model of the viscous sublayer. This model is of considerable intuitive appeal and fits well with visual observations of penetration of the wall region by turbulent fluctuations [2–8]. While such a highly simplified model cannot adequately describe essentially turbulent quantities such as the velocity fluctuations or the eddy diffusivity near the wall, it does allow solution of turbulent transport problems since said transport is assumed to occur under essentially viscous flow situations for which the governing differential equations and coefficients are well known.

Recently the periodic viscous sublayer model has been developed in detail and validating experimental evidence has been presented [9–11]. In the present paper heat-transfer coefficients for turbulently flowing fluids are calculated. After briefly describing the model we first make heat transfer calculations for $N_{Pr} > 1$ fluids in turbulent pipe flow based on simple boundary conditions and then discuss the case of liquid metals ($N_{Pr} \sim 0{\cdot}01$). Finally we present numerically calculated heat-transfer coefficients taking into account wall properties and a finite minimum turbulence penetration thickness.

THE VISCOUS SUBLAYER MODEL

The principal features of the intermittent or partial turbulence model are as follows:

1. At any time, the surfaces bounding a turbulent shear-flow field are covered with patches (sublayer elements) in unsteady-state viscous flow.
2. The velocity, u_B, at the outer edge of a given patch is essentially constant, and the growth in thickness of the element in time is treated as a semi-infinite boundary layer-type phenomenon.
3. The thickness of a patch, δ, increases with time until a viscous-turbulent transition takes place when $\delta = \delta_M$. The element then breaks up into a turbulent hash and mixes with the turbulent core.
4. The patch is replaced, essentially instantaneously, with another developing patch. The Einstein–Li assumption was that the development at the wall started from zero thickness. The physically more plausible assumption of decay to a fixed minimum thickness, δ_1, is introduced here.
5. The outer bounding velocity of a sublayer element, u_B, is determined in a self-consistent manner by continuity requirements. Einstein and Li arbitrarily assumed the bounding velocity to correspond to the velocity at a fixed distance from the wall. Mixing length theory is assumed to apply in the turbulent core.

If the transition criterion of the viscous sublayer element were known, the parameters arising in the model—such as the growth period and the maximum sublayer thickness—could, in principle, be calculated directly from a knowledge only of the velocity distribution in the fully turbulent core. Such a criterion is not available, and one experimental relationship—the Prandtl correlation for the friction factor as a function of the Reynolds number—was introduced to permit completion of the model [9, 10]. It is further assumed that a mean growth and decay period can be defined which is representative of this random process.

A mean dimensionless sublayer growth period, $T^+ = u_*(T/\nu)^{\frac{1}{2}}$ can be calculated [9, 10] based upon this model. Here T is the actual growth and decay period. For Reynolds numbers greater than 10^4, T^+ is substantially constant

and equals 18. Experimental, average-growth-period data supporting the calculations are presented elsewhere [9–11].

We also note here that, based on the same physical picture as is the Einstein–Li [1] model, Black [12, 13] has proposed a theory in which wall turbulence is viewed as an organized, time-dependent, viscosity governed, primary motion which becomes unstable and breaks down periodically in space and time to generate and maintain a system of characteristic horseshoe vortex structures which are intimately coupled to the temporal and spatial behavior of the sublayer. By making a number of assumptions [12] Black's model simplifies to the Einstein–Li case so that it may be thought of as a limiting case of Black's more complex, and more realistic, theory. Two of the principal defects of the simple model are that the sublayer thickness does not arise naturally but is treated in the "boundary-layer" formalism and that the transition criterion is unknown. It is hoped that the more complex model of Black will be of aid in this regard. In point of fact, however, the present version of the model is extremely successful in predicting heat and mass transport if the momentum transport (that is the friction factor) is known.

HEAT TRANSFER WITH SIMPLE BOUNDARY CONDITIONS

Heat transfer coefficients, $N_{Pr} > 1$

When it is assumed that the thermal conductivity is constant, that the axial and transverse temperature variations are negligible, that the viscous dissipation is negligible, and that the problem can be adequately described in cartesian coordinates, (sublayer thickness much less than pipe radius) then the equation of energy [14] becomes

$$\frac{\partial\theta}{\partial t} = \alpha\frac{\partial^2\theta}{\partial y^2}. \tag{1}$$

For the present, semi-infinite boundary conditions and turbulent penetration completely to the wall during the decay process will be assumed. Then the initial condition is

$$t = 0: y \geqslant 0, \theta = \theta_i, \tag{2}$$

and the first boundary condition on the temperature is

$$t = 0: y \to \infty, \theta = \theta_i, \tag{3}$$

where θ_i is a "boundary-layer" temperature analogous to the bounding velocity at the outer edge of the sublayer and is to be determined in a self-consistent manner. Two wall conditions are of interest, namely constant wall temperature and constant wall flux. The solution to (2) with (3) and (4) is well known in either case [15].

In the turbulent core, only time averaged quantities are considered and mixing length theory is applied. The temperature distribution in the core, suitably matched to the average sublayer temperature distribution is [9]

$$\bar{\theta} = -\frac{\bar{q}_w\alpha}{u_*k\kappa}\ln\left(\frac{y}{\delta_M}\right) + \theta_i, N_{Pr} > 1 \tag{4}$$

where $\kappa \equiv 0{\cdot}4$.

A local heat transfer coefficient defined by

$$\bar{q}_w \equiv h(\bar{\theta}_w - \langle\theta\rangle) \tag{5}$$

may now be calculated. The results [9] are plotted in Fig. 1. First, it is comforting to note that there is no really significant difference between the results obtained for the Stanton

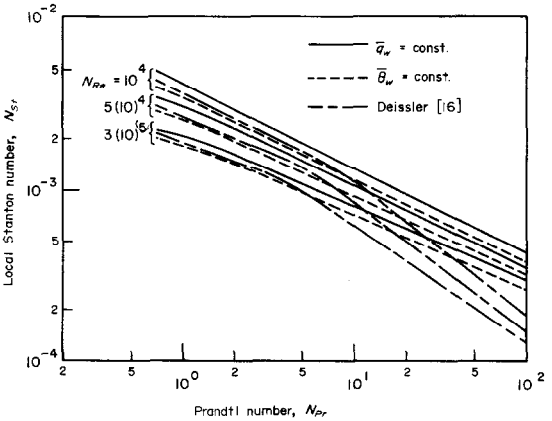

FIG. 1. Comparison of local Stanton numbers calculated from simple boundary conditions with Deissler's correlation.

number from the two different boundary conditions. However, from comparison with Deissler's correlation [16], it is seen that the calculated values are substantially in error for $N_{Pr} > 10$.

A discrepancy might have been anticipated. In the first place neither the constant wall temperature nor constant flux can correspond to reality, since the sublayer oscillations impose a wall temperature fluctuation and the wall temperature and heat transfer problems must be solved simultaneously. Secondly, the turbulent fluctuations almost certainly do not penetrate completely to the wall but to only a minimum thickness value, δ_1. Both these features are taken into account in a numerical method of solution to be presented later in this paper. These simple solutions are, however, of interest and use for moderate values of the Prandtl number.

In developing the viscous sublayer flow model, the sublayer thickness was defined as the point where the velocity becomes 99 per cent of the bounding velocity u_B [9, 10]. For the error function velocity profile this led to [9, 10]

$$\delta = 3{\cdot}64(\nu t)^{\frac{1}{2}} \tag{6}$$

and to a value for $\delta_M^+ = 65$ for the maximum thickness at $t = T$ when $T^+ = 18$.

By analogy to the sublayer thickness, a thermal thickness, δ_T, is defined such that

$$\theta(0, t) - \theta(\delta_T, t) = 0{\cdot}99(\theta(0, t) - \theta_i).$$

For constant wall flux this leads to

$$\delta_T = c_T(\alpha t)^{\frac{1}{2}} \tag{7}$$

where $c_T = 3{\cdot}20$ or $3{\cdot}64$ for the constant flux or constant wall temperature cases respectively.

For Prandtl numbers greater than one, the thermal thickness is less than the sublayer thickness, so that treating the heat transfer problem in the boundary layer formalism with $\theta \to \theta_i$ as $y \to \infty$ is satisfactory.

Liquid metals, $N_{Pr} < 1$

For Prandtl numbers less than one, the thermal thickness is greater than the sublayer thickness. Two difficulties must be considered. The first concerns the applicability of the initial condition and the second the accuracy of the computed flux. If the initial condition, equation (2), is to apply we must introduce the additional assumption that during the (assumed negligibly short) sublayer breakup time, the eddy thermal diffusivity is much greater than the molecular thermal diffusivity so that the sublayer fluid is mixed thoroughly into the turbulent core. In the liquid metal case this is not a very plausible assumption but is necessary in order to apply this model in this case. Calculations are made and a comparison to experimental data is presented to determine the validity of this approach in the low Prandtl number situation.

When the thermal wave extends beyond the growing viscous sublayer, the heat transfer in the turbulent region, $\delta < y$, must be considered. Since the eddy thermal diffusivity in this region is position (and likely time) dependent, an analytical evaluation of this effect can only be made in terms of average properties of the transport coefficients in this region. In the following, the turbulent eddy transport coefficients, α_t and ν_t, were evaluated at the time average value of the thermal wave thickness, i.e. $\frac{2}{3}$ of the thickness, $\delta_{T_m}^+$, given by equation (7) in dimensionless form at T^+. The value of the eddy diffusivity for momentum transport, ν_t, was obtained at this thickness from the Reichart relationship [17] and the ratio α_t/ν_t from the Jenkins' calculation [18] was used to evaluate α_t.

If an essentially constant value for α_t is adequate for $y > \delta$, the heat flux at the wall, q_w, for constant θ_w is obtained by solution of the one dimensional transient heat conduction equation in the regions $0 < y < \delta(t)$ with molecular transport coefficients and $\delta(t) < y^+ < \infty$ with the sum of the molecular and turbulent coefficients. The ρc product would be the same in both regions. Since the boundary $\delta(t)$ increases with time, this problem is similar to the so called classical Stefan–Neumann or "ice formation" problem. In the present problem the functional

dependence of $\delta(t)$ is known, equation (6), and the temperature distribution can be obtained by a combination of variables as was done by Ruoff [19] for the ice melting problem. If q_0 is the heat flux computed for molecular properties extending to $y \to \infty$, which is the case obtained from the periodic model, the ratio

$$\frac{q_w}{q_0} = \frac{1}{\operatorname{erf} \xi_1 + \beta \operatorname{erfc} \xi_2} \tag{8}$$

can be obtained. Here, $\xi_1 = 1{\cdot}82\ (N_{Pr})^{\frac{1}{2}}$, $\xi_2 = 1{\cdot}82\ R_\Gamma (N_{Pr})^{1/2}$, $\beta = R_\Gamma \exp(\xi_2^2 - \xi_1^2)$, and

$$R_\Gamma = \left(\frac{k}{k_t + k}\right)^{1/2} = \left(\frac{\alpha}{\alpha_t + \alpha}\right)^{1/2}.$$

Equation (8) predicts no effect of the thermal wave penetration beyond δ for $N_{Pr} \to 0$ because the turbulent mechanism would be dominated by molecular conduction and also no effect for $N_{Pr} \to 1$ since the thermal wave penetration would be negligible. For typical values of α_t/α the maximum effect occurs at $N_{Pr} \cong 0{\cdot}04$. For $N_{Pr} = 0{\cdot}005$, which corresponds to the alkali metal liquids, thermal wave penetration at T is great enough that the average value of $\nu_t/\nu \cong 200$ and the Jenkins' correction $\alpha_t/\nu_t \cong 0{\cdot}17$. For $N_{Pr} = 0{\cdot}03$, which corresponds to a heavy metal such as mercury, the average value of $\nu_t/\nu \cong 100$ and $\alpha_t/\nu_t \cong 0{\cdot}35$. In each case and over the range of Prandtl numbers of interest, it is found that $R_\Gamma \cong 1/(35N_{Pr} + 1)$. At $N_{Pr} = 0{\cdot}005$, q_w is within 10 per cent of q_0, and to an adequate approximation the effect of the heat flow in the two types of regions may be neglected. For $N_{Pr} = 0{\cdot}03$, $q_w \cong 1{\cdot}25 q_0$ and a significant correction for the high conductivity region δ must be considered.

Quantitative evaluation of heat transfer coefficients will be delayed to the section on numerical calculation. However, it is noted here that the velocity and temperature profiles are needed in the turbulent core for the evaluation of $\langle\theta\rangle$ and hence the heat transfer coefficient. In the case of the large Prandtl number fluids, equation (4) was used for temperature and

$$u_z = \frac{u_*}{\kappa} \ln\left(\frac{y}{\delta_M}\right) + 0{\cdot}99\, u_B \tag{9}$$

was used for velocity [9, 10]. The latter is also used for the liquid metal case as is justified by experiment [20].

However, equation (4) does not apply as is made amply clear in the preceding argument concerning α_t/α. Rather both molecular and turbulent transport must be considered in the core. Furthermore, it was seen that the sublayer temperature oscillations extend into the core. (This should be experimentally observable.) Therefore, in the region $\delta_M < y < \delta_{TM}$ no truly rational method exists for computing the temperature profile within the framework of the simplified model. In particular we will introduce a second additional assumption that outside the sublayer, $y < \delta_M$, it is satisfactory to use a time averaged temperature profile matched to $\bar{\theta}(\delta_M)$ at $y = \delta_M$. That is

$$\bar{\theta} = \bar{\theta}(\delta_M) - \frac{\bar{q}_w}{\rho c u_*} \int_{\delta_M^+}^{y^+} \frac{\left(1 - \dfrac{y^+}{R^+}\right) \mathrm{d}y^+}{\kappa y^+ \left(1 - \dfrac{y^+}{R^+}\right) + \dfrac{1}{N_{Pr}}} \tag{10}$$

$$N_{Pr} < 1.$$

Mixing length theory is used for the turbulent transport contribution and axial transport is neglected as was done in deriving equation (4). The further implication of this will be discussed later.

Temperature profiles

It is of interest to compare not only heat-transfer coefficients but also temperature profiles with experiment. For moderate and low Prandtl numbers the analytical solutions give satisfactory results. A dimensionless temperature is defined by

$$\overline{\theta^+} = \frac{\bar{\theta}_w - \theta}{\bar{q}_w} \rho c u_*. \tag{11}$$

Equation (4) which applies in the core and the analytical expressions for the mean temperatures in the sublayer may be integrated analytically, by successive integrations by parts. The results are

$$\overline{\theta^+} = \frac{N_{Pr}^{\frac{3}{2}} y^{+2}}{3\pi^{\frac{1}{2}} T^+} \exp(-y^{+2} N_{Pr}/4T^{+2}) - y^+ N_{Pr} \operatorname{erfc}(y^+ N_{Pr}^{\frac{1}{2}}/2T^+) - \frac{y^{+3} N_{Pr}}{6T^{+2}} \operatorname{erfc}(y^+ N_{Pr}^{\frac{1}{2}}/2T^+) + \frac{4N_{Pr}^{\frac{1}{2}} T^+}{3\pi^{\frac{1}{2}}} \left[\exp(-y^{+2} N_{Pr}/4T^{+2}) - 1\right], \quad q_w = \text{const.} \tag{12}$$

and

$$\overline{\theta^+} = \frac{\pi^{\frac{1}{2}} N_{Pr}^{\frac{1}{2}}}{2} T^+ \operatorname{erf}(Y^+ N_{Pr}^{\frac{1}{2}}/2T^+) - \frac{N_{Pr} y^+}{2} \exp(-y^{+2} N_{Pr}/4T^{+2}) - \frac{\pi^{\frac{1}{2}} N_{Pr}^{\frac{3}{2}} y^{+2}}{4T^+} \operatorname{erfc}(y^+ N_{Pr}^{\frac{1}{2}}/2T^+), \theta_w = \text{const.} \tag{13}$$

These results depend on the Reynolds number only through T^+ which is substantially constant for $N_{Re} > 10^4$. Furthermore, the profiles from (12) and (13) do not differ appreciably. Comparison to experimental data [20, 22–24] is made in Fig. 2 where the magnitude of the maximum sublayer thickness and the maximum thermal thickness are also indicated. The agreement is adequate. Thomas [21] has discussed temperature profiles from the periodic viscous sublayer viewpoint, although he prefers to speak in surface renewal terminology. Thomas [21] however, used an empirical surface age distribution and took $u_B = \langle u \rangle$ which is not consistent with continuity requirements [9, 10].

A restriction upon the Reynolds number range which it is strictly legitimate to consider now becomes apparent. For a given value of N_{Pr} there is a minimum value of R^+ for meaningful results, since these calculations have been

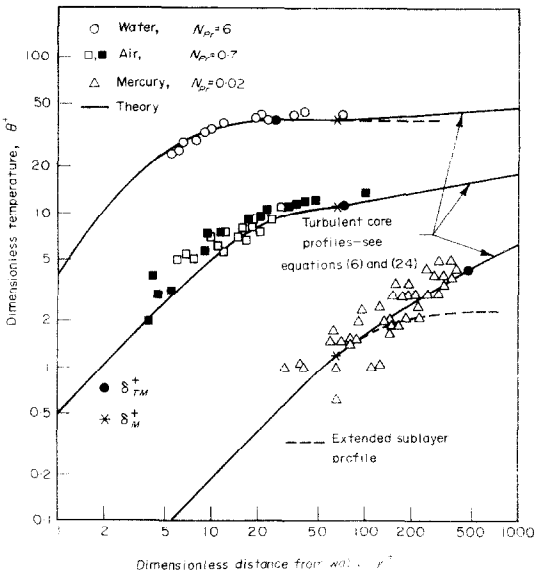

FIG. 2. Calculated dimensionless temperature as a function of dimensionless distance from the wall for comparison with experimental data at various fluid Prandtl numbers. Data for water are from [22], for air are from [23, 24] and for mercury are from [20].

set up in cartesian coordinates. R^+ must be significantly greater than δ^+. If $\delta_M^+ = 65$, the Fanning friction factor is about 0·0045, and R^+ is taken as twice δ_{TM}^+, it is found that $N_{Pe} \gtrsim 5{\cdot}5(10^3) N_{Pr}^{\frac{1}{2}}$ [9, 10]. A similar requirement is needed because of neglect of axial transport. Experimental data indicate lack of dependence on the axial boundary condition only for $N_{Pe} \gtrsim 100$ [25].

NUMERICAL SOLUTION OF THE HEAT WALL PROBLEM

As was mentioned above, the simple solutions presented thus far neglect two important physical phenomena. First, since sublayer oscillations impose wall temperature fluctuations, the temperature distribution in wall and sublayer must be solved simultaneously. Second, during transition of the sublayer element, turbulent fluctuations do not penetrate completely to the wall but rather only to some minimum sublayer thickness δ_1. (The data of Popovich and Hummel

[5] indicate that $\delta_1^+ = 1{\cdot}6 \pm 0{\cdot}4$.) It has been shown [9, 10] that introduction of such a minimum thickness is very important in heat-transfer determinations at large Prandtl numbers where a significant portion of the temperature drop may occur for $y < \delta_1$; that is where δ_{TM} becomes of the order of or less than δ_1.

The numerical method

If a wall which is transferring heat to a fluctuating viscous sublayer is so thick that significant fluctuations in temperature do not penetrate it, a convenient mathematical description of the heat-transfer process may be formulated as follows:

For $y < 0$ (into the wall), the differential equation is the same as equation (1). Since the sublayer oscillations have average period T, it is clear that the solution desired in this case is such that

$$\theta(y, t + T) = \theta(y, T). \tag{14}$$

The initial starting solution necessary is taken to be

$$t = 0: y \leqslant 0, \theta = -\bar{q}_w y + \bar{\theta}_w, \tag{15}$$

where $\bar{q}_w$ is estimated in a manner to be described shortly. The boundary condition on the wall is

$$\text{all } t: y \to -\infty, -k_s \frac{\partial \theta}{\partial y} = \bar{q}_w \equiv h(\bar{\theta}_w - \langle\theta\rangle) \tag{16}$$

where the final identity introduces the heat-transfer coefficient, h.

For $y \geqslant 0$ (in the fluid), equation (1) still applies. The initial and boundary conditions for the fluid may be written as

$$t = nT: \text{all } y > \delta_1, \theta = \theta_i; \tag{17}$$

and

$$t > 0: y \to \infty, \theta = \theta_i. \tag{18}$$

For $y = 0$ (at the solid–fluid interface), continuity of temperature and flux gives

$$\theta(-\varepsilon, t) = \theta(\varepsilon, t) \tag{19}$$

and

$$k_s \frac{\partial \theta}{\partial y}(-\varepsilon, t) = k \frac{\partial \theta}{\partial y}(\varepsilon, t). \tag{20}$$

Calculations are begun by use of equation (15); as n—the number of times the sublayer grows and decays—becomes large, the calculated temperature oscillations converge to steady periodic values and thus wall temperature fluctuations and average heat-transfer coefficients which can be compared with experiments are calculated.

Before the method of solution is detailed, it is advantageous to perform a simple dimensional analysis [9]. The result is

$$N_{Nu} = N_{Nu}\left(N_{Re}, N_{Pr}, \frac{\alpha}{\alpha_s}, \frac{\Gamma}{\Gamma_s}\right) \tag{21}$$

and

$$\frac{(\overline{\theta_w'^2})^{\frac{1}{2}}}{\bar{\theta}_w - \langle\theta\rangle} = g\left(N_{Re}, N_{Pr}, \frac{\alpha}{\alpha_s}, \frac{\Gamma}{\Gamma_s}\right). \tag{22}$$

It is expected, from knowledge of experiments, that the effects of (α/α_s) and (Γ/Γ_s) on N_{Nu} are small while, intuitively, it seems possible that their effects on the relative RMS wall temperature fluctuation may be significant. These allegations are borne out by the results of calculations for various wall and fluid properties [9].

For the numerical solution, the equations were rewritten in terms of dimensionless variables by combination with the solid thermal properties, with the period, and with an estimated mean interface-to-fluid temperature difference. The mean heat flux and this temperature difference were calculated from an estimated heat-transfer coefficient. If the estimated coefficient was exact, the time-averaged surface temperature from a calculation was 1·0; otherwise, the interface value approached some value near to the one as the number of simulated cycles was increased.

The period, T, can be calculated from the fluid properties if T^+ and $\langle u_z^+ \rangle$ are known. The values of these dimensionless variables

[9, 10] have been calculated and can be represented adequately by

$$T^+ = \gamma^{-1} + 17{\cdot}6, \tag{23}$$

where

$$\gamma = 0{\cdot}6 \ln N_{Re} - 0{\cdot}00965 (\ln N_{Re})^2 - 3{\cdot}78, \tag{24}$$

and by

$$\langle u_z^+ \rangle = 1{\cdot}84 \ln N_{Re} + 0{\cdot}0158 (\ln N_{Re})^2 - 2{\cdot}18. \tag{25}$$

The semi-infinite boundary conditions were approximated for the numerical solution by specification of the conditions at some distance from the interface. For the solid, the constant mean heat flux was imposed at a distance at which the temperature fluctuation would be less than one per cent of sinusoidal surface-temperature fluctuations at a frequency corresponding to the growth period. For the fluid, the dimensionless temperature was set equal to zero at such a distance that the temperature change during a single period would be less than ten per cent of the surface-temperature change. The continuity conditions at the interface were satisfied by use of fictitious temperatures on either side of the interface.

The differential equations were put into the form of the Crank–Nicholson six-point implicit representation [26] for the numerical calculations. Since this representation yields a tridiagonal matrix for general interior points, the finite difference equations from the boundary condition approximations were also placed in tridiagonal form; and the temperature distributions within the solid and the fluid were calculated for successive increments by inversion of the tridiagonal matrix by the method of Thomas [26].

The numerical solution was checked against the analytical solutions which can be developed for the first growth period, and the maximum difference between calculated temperature profiles was less than one per cent. No significant changes in the solution were obtained when the spatial or time increments were changed by factors of ten nor when double-precision calculations were made. Normally, after 20 simulated periods, the calculated relative RMS temperature fluctuations were varying less than $\frac{1}{10}$ per cent per period. Fast convergence to a steady-state heat-transfer coefficient was achieved when the solution was restarted after 10 periods with this numerically determined coefficient used as the estimate for the starting solution.

Input data to the program were the Reynolds number, the tube diameter, and the thermal properties of the wall and fluid, while the output includes the Nusselt or Stanton number and the relative RMS wall-temperature fluctuation. Calculated values are compared to experimental values in the following sections.

The numerical solution yielded results in terms of a Stanton number (N'_{St}) based on the temperature difference $\bar{\theta}_w - \theta_i$ rather than the more useful Stanton number (N_{St}) based on the difference $\langle\theta\rangle - \bar{\theta}_w$. In general, a numerical integration is required to obtain the ratio $N_{St}/N'_{St} = (\langle\theta\rangle - \bar{\theta}_w)/(\bar{\theta}_w - \theta_i)$; however, a practical approximation can be obtained if a logarithmic temperature distribution is assumed for the turbulent core and the value $\bar{\theta}_w - \theta_i$ given by equation (4) is employed to give θ_i at δ_M^+. It is thus possible to show that [9]

$$N_{St} = \frac{N'_{St}}{1 + \alpha N'_{St}}, \text{ where} \tag{26}$$

$$\alpha = \frac{1}{\kappa^2}(\ln^2 Z - 3 \ln Z + 3{\cdot}5) - \frac{0{\cdot}99 u_B^+}{\kappa} (\ln Z - 1{\cdot}5); \tag{27}$$

$$Z = R^+/\delta_M^+.$$

For N_{Re} greater than 9000, equation (27) can be represented in terms of N_{Re} as $\alpha = (-39{\cdot}8 + 4{\cdot}1854 \ln N_{Re}) \ln N_{Re} + 21{\cdot}04$.

Wall temperature fluctuations

Extensive wall temperature fluctuation measurements have been made [9] and reported elsewhere [10]. Mean periods were determined by autocorrelation and found to correspond

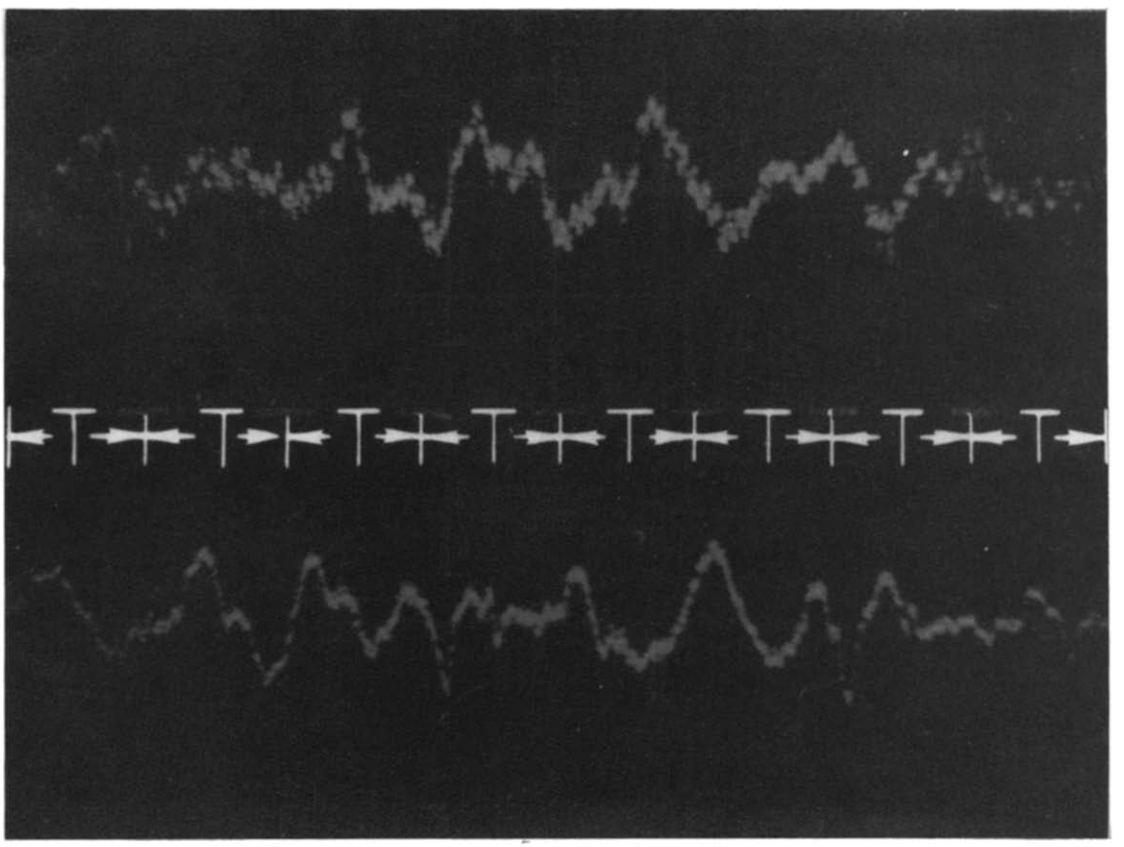

FIG. 4. Measured wall-temperature fluctuations from a pair of sensors in a Pyrex tube for Tetralin at $N_{Re} = 3(10)^4$. The horizontal time scale is 160 ms per major division. The period T indicated is that found from autocorrelation of the signal.

well to theoretical values of the mean period. Wall temperature fluctuation magnitudes may be compared to the calculations outlined above.

Calculated wall-temperature wave forms for various assumed values of the minimum thickness, δ_1, are plotted in Fig. 3 for Tetralin in a

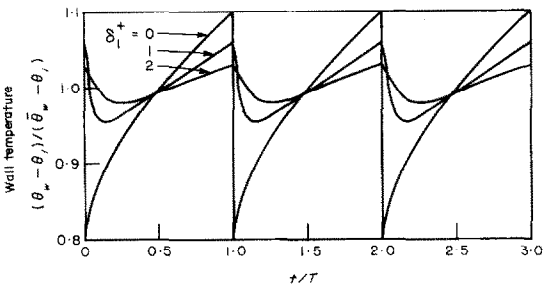

FIG. 3. Numerically computed wall-temperature oscillations for Tetralin in a Pyrex tube at $N_{Re} = 5(10)^4$.

Pyrex tube at a Reynolds number of $5(10)^4$. This may be compared to Fig. 4 which is an oscilloscope trace of wall temperature fluctuations from a pair of platinum-film wall-temperature sensors [9, 10] in a Pyrex tube for Tetralin at a Reynolds number of $3(10)^4$ [9, 10]. The period, T, indicated in Fig. 4 is that determined from autocorrelation. Of course, it must be

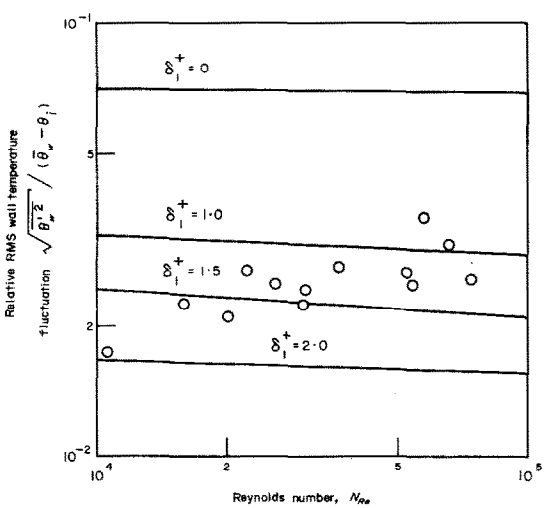

FIG. 5. RMS wall-temperature fluctuations for Tetralin in Pyrex tubes for comparison with calculated values for various minimum sublayer thicknesses.

remembered that T as determined from the model is only an average of a statistical quantity.

Figure 5 compares experimental relative RMS wall temperature fluctuations for Tetralin in Pyrex tubes [9, 10] to those computed for various assumed minimum thickness values.

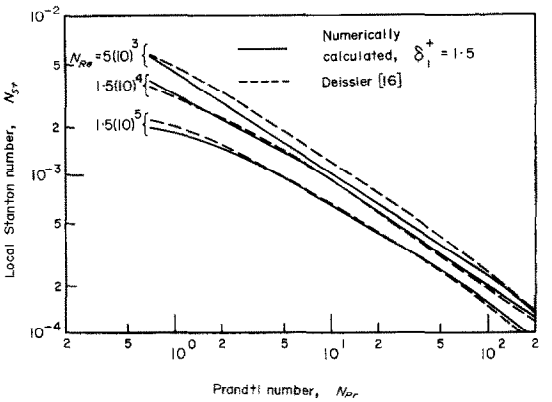

FIG. 6. Numerically computed local Stanton number as a function of Reynolds and Prandtl number compared to Deissler's correlation for Prandtl numbers greater than unity.

Good agreement is obtained for $\delta_1^+ = 1{\cdot}5$, which is essentially the value found experimentally by Popovich and Hummel [4, 5], and it was also found that this value gave the best heat-transfer coefficients.

Heat-transfer coefficients

Computed values of the Stanton number for Prandtl numbers greater than one are plotted in Fig. 6 for various Reynolds numbers and a dimensionless minimum thickness of 1·5. Comparison to Deissler's correlation [16] is made and agreement within the estimated accuracy of the empirical correlation is obtained to Prandtl numbers of one to two hundred for Reynolds numbers of 10^4 or greater. In the transition region $N_{Re} < 10^4$, some discrepancy is probably introduced by use of sublayer solutions strictly applicable to parallel plate, not tube, geometries [9]. In the case of very high Prandtl number fluids, the deviation between prediction and the Deissler correlation is significant. For $N_{Pr} = 1000$

and 3000 the predicted values of N_{St} are 20 and 35 per cent low respectively.

For Prandtl numbers less than one, liquid metals, two empirical correlations have attained rather wide acceptance. A number of heat-transfer texts (e.g. [27, 28]) give an empirical equation due to Lubarsky and Kaufman [29]

$$N_{Nu} = 0{\cdot}625\,(N_{Re}\,N_{Pr})^{0{\cdot}4}, \qquad (28)$$

while the *Chemical Engineers Handbook* [30] recommends [31]

$$N_{Nu} = 5{\cdot}0 + 0{\cdot}016\,(N_{Re}\,N_{Pr})^{0{\cdot}8} \qquad (29)$$

which is of the Martenelli [32]–Lyon [33] form, but with empirical coefficients. Both equations (27) and (28) are plotted in Fig. 7. It should be

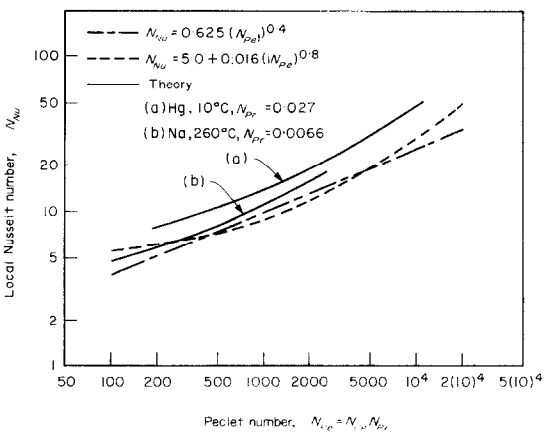

FIG. 7. Numerically computed local Nusselt numbers for mercury and sodium in stainless steel tubes are compared to empirical correlations. The curve for the mercury calculation should be increased by about 25 per cent as required by equation (8). The data correlations are from [29] and [31].

noted that the experimental data upon which these correlations are based deviated ± 25 per cent from their mean.

The results of numerical calculations for Na at 500°F and Hg at 50°F flowing in stainless steel tubes are also plotted in Fig. 7. The Prandtl numbers were 0·0066 and 0·027 respectively. The position of the curve from the Hg calculation should be raised by approximately 25 per cent as required by equation (8) because of the effect of turbulent transport in the region beyond the edge of the fluid dynamic boundary layer. The simple periodic boundary layer model is not really adequate for treatment of heat transfer of the intermediate Prandtl number fluids ($0{\cdot}01 \lesssim N_{Pr} \lesssim 0{\cdot}2$). The computed heat-transfer coefficients for the Na case are in reasonable agreement correlations and average about 25 per cent high. Agreement is also good at low Péclét numbers which is rather surprising in light of the arguments of the preceding sections. Rather large wall-temperature fluctuations should be produced by the sublayer growth and decay. The relative values were calculated to be 10 and 17 per cent for the Na and Hg respectively. As a result, the computations indicate a dependence on Prandtl number of the N_{Nu} vs Péclét number relationship. This may be a real effect, which should be tested by careful experiments, and may in fact explain some of what has previously appeared to be scatter in the data.

SUMMARY AND CONCLUSIONS

The simple model of the periodically growing and decaying turbulent boundary layer was found to predict fully-developed turbulent heat-transfer relationships in agreement with previously presented correlations over a wide range of conditions. Turbulent-flow heat-transfer rates are calculated by use of relationships obtained by solution to the one-dimensional heat conduction equation. Processes in the turbulent core are assumed to be describable by simple mixing length theory. The boundary layer growth periods are obtained from fluid dynamic considerations, and the Prandtl friction factor law is assumed to apply. Since the fluid dynamic considerations supply a critical parameter to the model, the approach described is really a fluid-heat transfer analogy in a somewhat unconventional sense.

For Prandtl numbers greater than about 0·7 and less than 200, and Reynolds numbers greater than 5000, the predictions of the periodic

sublayer model are in practical agreement with the calculations of Deissler [16] and Kays [34]. A significant discrepancy between prediction and experiment is noted for the very high Prandtl number (really high Schmidt number) fluids. This discrepancy is likely the result of treating the region from $0 < y < \delta_1$ as laminar and neglecting the minute, but still significant eddy diffusion very close to the wall.

Agreement between calculation and experiment for the very low Prandtl number fluids is obtained by use of a time averaged temperature profile in the turbulent core which is matched to the assumed constant temperature of the growing thermal boundary layer at the maximum growth thickness of the fluid boundary layer. The low Prandtl number calculations were not intended to be of a predictive nature and are presented to show that in this case reasonable agreement between calculation and observation could be obtained by use of plausible assumptions.

The major advantages of the approach discussed for computation of turbulent heat transfer here is the straightforward nature of the calculations which employ a simple, heuristically attractive model of the sublayer. The only experimentally undefined parameter needed is the mean, minimum decay thickness of the sublayer, and the value of 1·5 in law of the wall units employed in these calculations was found to be consistent with the values obtained by measurement of the wall temperature fluctuations during turbulent heat transfer [10, 11].

ACKNOWLEDGEMENT

This work was supported by the National Science Foundation under Grants GK-1357 and GK-10114.

REFERENCES

1. H. A. EINSTEIN and H. LI, The viscous sub-layer along a smooth boundary, *Am. Soc. Civil Engrs* **82**, 293 (1956).
2. A. FAGE and H. C. H. TOWNEND, An examination of turbulent flow with an ultramicroscope, *Proc. R. Soc., Lond.* **135A**, 656 (1932). See also: G. I. TAYLOR, Note a solid wall, *Proc. R. Soc., Lond.* **135A**, 678 (1932).
3. S. J. KLINE and P. W. RUNSTADLER, Some preliminary results of visual studies of the flow model of the wall layers of the turbulent boundary layer, *J. Appl. Mech.* **81E**, 166 (1959).
4. A. T. POPOVICH and R. L. HUMMEL, A new method for non-disrupting turbulent flow measurements very close to a wall, *Chem. Engr. Sci.* **22**, 21 (1967).
5. A. T. POPOVICH and R. L. HUMMEL, Experimental study of the viscous sublayer in turbulent pipe flow, *A.I.Ch.E. Jl* **13**, 854 (1967).
6. P. W. RUNSTADLER, S. J. KLINE and W. C. REYNOLDS, An experimental investigation of the flow structure of the turbulent boundary layer, MD-8; Dept. of Mech. Engng, Stanford University (1963).
7. F. A. SCHRAUB and S. J. KLINE, A study of the turbulent boundary layer with and without longitudinal pressure gradients, MD-12; Dept. of Mech. Engr., Stanford University (1965).
8. E. R. CORINO and R. S. BRODKEY, A visual investigation of the wall region in turbulent flow, *J. Fluid Mech.* **37**, 1 (1969).
9. R. L. MEEK, A study of the viscous sublayer in turbulent flow, Ph.D. Thesis, University of Utah, Salt Lake City (June 1968).
10. R. L. MEEK and A. D. BAER, The periodic viscous sublayer in turbulent flow, *A.I.Ch.E. Jl* **16**, 841 (1970).
11. R. L. MEEK and A. D. BAER, The periodic viscous sublayer model and heat transfer to drag-reducing solutions, *A.I.Ch.E. Jl.* **16**, 1100 (1970).
12. T. J. BLACK, A new model of the shear stress mechanism in wall turbulence, AIAA 6th Aero. Sci. Meeting, AIAA No. 68–42 (1968).
13. T. J. BLACK, Viscous drag reduction examined in the light of a new model of wall turbulence. *Viscous Drag Reduction*, edited by C. S. WELLS, p. 383. Plenum Press, New York (1969).
14. R. B. BIRD, W. E. STEWART and E. N. LIGHTFOOT, *Transport Phenomena*. John Wiley, New York (1960).
15. H. S. CARSLAW and J. C. JAEGER, *Conduction of Heat in Solids*. Oxford University Press, London (1959).
16. R. G. DEISSLER, Analysis of turbulent heat transfer, mass transfer and friction in smooth tubes at high Prandtl and Schmidt numbers, *Recent Advances in Heat and Mass Transfer*, edited by J. P. HARTNETT, p. 253. McGraw-Hill, New York (1961).
17. H. REICHARDT, The principles of turbulent heat transfer, *Recent Advances in Heat and Mass Transfer*, edited by J. P. HARTNETT, p. 223. McGraw-Hill, New York (1961).
18. R. JENKINS, Variation of the eddy conductivity with Prandtl number and its use in the prediction of turbulent heat transfer coefficients, *Heat Transfer and Fluid Mechanics Inst.*, Stanford University Press, p. 147 (1951).
19. A. L. RUOFF, An alternate solution of Stefan's problem, *Q. J. Appl. Math.* **16**, 197 (1958).
20. H. E. BROWN, B. H. AMSTEAD and B. E. SHORT, Temperature and velocity distribution and transfer of heat in a liquid metal, *Trans. ASME* **79**, 279 (1957).
21. L. C. THOMAS, Temperature profiles for liquid metals and moderate-Prandtl-number fluids, *J. Heat Transfer*, **92**, 565 (1970).
22. R. A. GOWEN and J. W. SMITH, The effect of the Prandtl

number on temperature profiles for heat transfer in turbulent pipe flow, *Chem. Engng Sci.* **22**, 1701 (1967).
23. R. G. DEISSLER and C. S. EIEN, Analysis of turbulent heat transfer, mass transfer, and friction in smooth tubes at high Prandtl and Schmidt numbers, NACA TN 2629 (1952).
24. R. E. JOHNK and T. J. HANRATTY, Temperature profiles for turbulent flow of air in a pipe, *Chem. Engng Sci.* **17**, 881 (1962).
25. R. P. STEIN, Liquid metal heat transfer, *Advances in Heat Transfer*, Vol. 3, p. 101. Academic Press, New York (1966).
26. L. LAPIDUS, *Digital Computation for Chemical Engineers*, pp. 162, 254. McGraw-Hill, New York (1962).
27. F. KREITH, *Principles of Heat Transfer*, p. 351. International Textbook Company, Scranton (1962).
28. S. T. HSU, *Engineering Heat Transfer*, p. 308 Van Nostrand, Princeton (1963).
29. B. LUBARSKY and S. J. KAUFMAN, Review of experimental investigations of liquid metal heat transfer, NACA TN 3336 (1955).
30. J. H. PERRY *et. al.* (Eds.), *Chemical Engineers Handbook*, 4th Edition, p. 10–25. McGraw-Hill, New York (1963).
31. H. A. JOHNSON *et al.*, Heat transfer to mercury in turbulent pipe flow, *Trans. ASME* **76**, 505 (1954).
32. R. C. MARTENELLI, Heat transfer to molten metals, *Trans. ASME* **69**, 947 (1947).
33. R. N. LYON, Liquid-metal heat transfer coefficients, *Chem. Engng Prog.* **47**, 75 (1951).
34. W. M. KAYS, *Convective Heat and Mass Transfer*, p. 171. McGraw-Hill, New York (1966).

TRANSFERT DE CHALEUR TURBULENT ET SOUS-COUCHE VISQUEUSE PERIODIQUE

Résumé—On présente des calculs de transfert thermique basés sur le modèle de sous-couche visqueuse fluctuante d'un écoulement turbulent qui comprennent deux critères cependant négligeables de situation d'écoulement réelle, à savoir que les fluctuations de la sous-couche imposent des fluctuations de température pariétale et qu'en moyenne la sous-couche ne diminue pas complètement à la paroi mais qu'il existe plutôt une épaisseur maximale de pénétration de la turbulence. Les distributions de température résultantes et les coefficients de transfert thermique sont en accord avec les formules empiriques basées sur les résultats expérimentaux pour des nombres de Prandtl supérieur à un. Le transfert thermique pour des métaux liquides est aussi considéré (nombre de Prandtl bien inférieur à un) et les coefficients de transfert thermique calculés sont de 25 à 50% supérieurs à ceux des formules empiriques publiées. Ces calculs montrent que pour les métaux liquides le nombre de Nusselt n'est pas une fonction à valeur unique du nombre de Péclet.

TURBULENTE WÄRMEÜBERTRAGUNG UND DIE PERIODISCHE VISKOSE UNTERSCHICHT

Zusammenfassung—Mit dem Modell der "Schwankungen der viskosen Unterschicht" wurden Wärmeübergangsberechnungen bei turbulenter Strömung durchgeführt, die zwei wesentliche, aber früher vernachlässigte Merkmale der tatsächlichen Strömungssituation berücksichtigen, nämlich: daß Schwankungen der Unterschicht zu Schwankungen der Wandtemperatur führen und daß im Durchschnitt die Unterschicht zur Wand hin nicht vollständig verschwindet, sondern daß vielmehr eine minimale Turbulenz-Eindring-Dicke existiert. Die resultierenden Temperaturverteilungen und die Wärmeübergangskoeffizienten stimmen mit empirischen Korrelationen der experimentellen Daten für Prandtl-Zahlen grösser eins überein. Wärmeübergang bei Flüssigmetallen (Prandtl-Zahlen wesentlich kleiner als eins) wurde ebenfalls untersucht, die berechneten Wärmeübergangskoeffizienten liegen dabei um 25 bis 50% höher als veröffentlichte experimentelle Werte. Die Berechnungen zeigen, dass die Nusselt-Zahl für Flüssigmetalle keine eindeutige Funktion der Peclet-Zahl ist.

ТУРБУЛЕНТНЫЙ ТЕПЛООБМЕН И ПЕРИОДИЧЕСКИЙ ВЯЗКИЙ ПОДСЛОЙ

Аннотация—Приводятся расчеты теплообмена на основе модели турбулентного течения с пульсирующим вязким подслоем с учетом двух существенных, до этого пренебрегаемых особенностей реального течения, а именно: (1) флуктуации подслоя накладываются на флуктуации температуры стенки и (2) в среднем подслой полностью не затухает вблизи стенки, а скорее существует максимальная толщина проникновения турбулентности. Полученные профили температуры и коэффициенты теплообмена согласуются с экспериментальными данными при числах Прандтля больше единицы. Рассмотрен также перенос тепла к жидким металлам (число Прандтля гораздо меньше единицы). Расчетные значения коэффициентов теплообмена на 25–50% больше опубликованных в литературе экспериментальных данных. Расчеты показывают, что для жидких металлов число Нуссельта неоднозначно зависит от числа Пекле.